

# DESIGN STATUS OF THE MUNICH CYCLOTRON SUSE

H. DANIEL, G. GRAW, G. HINDERER, F. HINTERBERGER, E. HUENGES, P. KIENLE, H. J. KÖRNER, H. MORINAGA, E. NOLTE, H. J. SCHEERER, U. SCHNEIDER, W. SCHOTT, S. SKORKA, U. TRINKS, W. WIEDEMANN, W. WILHELM, E. ZECH, R. ZIERL

Physik-Department der Technischen Universität München and Sektion Physik der Universität München, Germany

## 1. Introduction

At the Munich Accelerator Laboratory a project study on a superconducting sector cyclotron (SuSe) with the existing 13 MV-tandem as injector is in progress. Fig. 1 shows the present layout of the combined system. SuSe will accelerate fully stripped ions with  $Q/A \geq 0.5$  ( $^1\text{H}$ ,  $^3\text{He}$ , ...  $^{32}\text{S}$ ) to the maximum energy of  $E/A = 300$  MeV/N and ions with  $Q/A$  as low as 0.16 ( $^{238}\text{U}^{38+}$ ) to  $E/A = 24$  MeV/N. Excellent beam qualities will be achieved by the tandem properties, the phase space matching and the phase compression due to the radial increase of the accelerating voltage. The data for some typical beams are given in Tab. 1. The main features of SuSe summarized in Tab. 2 hardly changed since the conference in 1979<sup>1</sup>. We report on some topics worked out in detail: the superconducting magnets, the RF-system and the beam transport and injection system.

The project study is funded by Bundesmin. f. Forsch.u. Techn. (FRG) and will be finished at the end of 1982. The project itself is recommended but not yet funded.

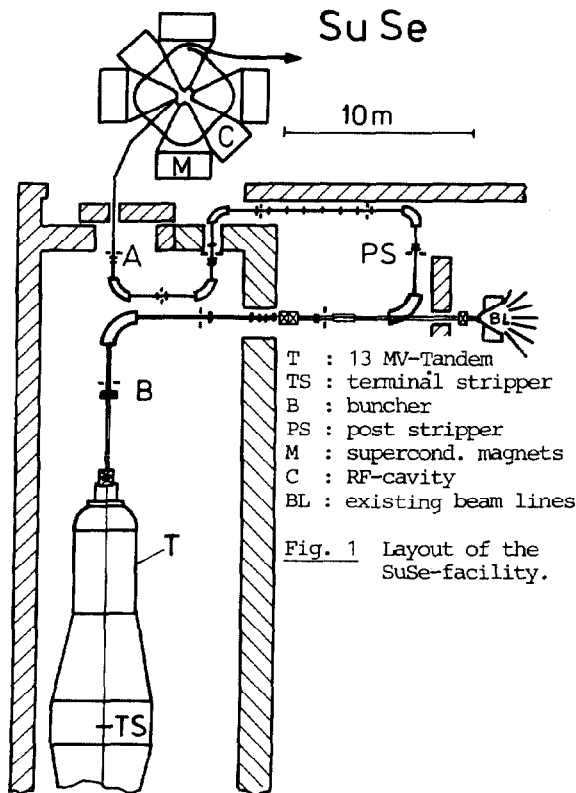


Table 1: Some properties of typical beams

Ion	$^{12}_6\text{C}^{6+}$	$^{32}_{16}\text{S}^{15+}$	$^{58}_{28}\text{Ni}^{21+}$	$^{197}_{79}\text{Au}^{34+}$
$E/A$ [MeV/N]	300	246	126	25
$\epsilon_{x,y}$ [mm mrad]	0.13	0.15	0.19	0.42
$\Delta E/E$ [ $10^{-4}$ ]	1.0	1.7	2.3	3.1
bunch [psec]	16	17	19	46
intensity [pnA]	3700	18	10	1

Table 2: Main features of SuSe

Injector	13 MV-tandem
Injection radius $r_1$	.40 m
Extraction radius $r_2$	2.40 m
Average field at $r_2$	2.25 T
Bending power $K_B$	1400
2 accelerating cavities,	TE 101 mode
Resonant frequency range	78.6 ... 49.6 MHz
Harmonic operation modes	6., 7., ... 16
Max. acc. Volt./cavity	1 MV
RF-power total	< 200 kW
beam separation at $r_1$	9.2 mm
beam separation at $r_2$	2.6 mm

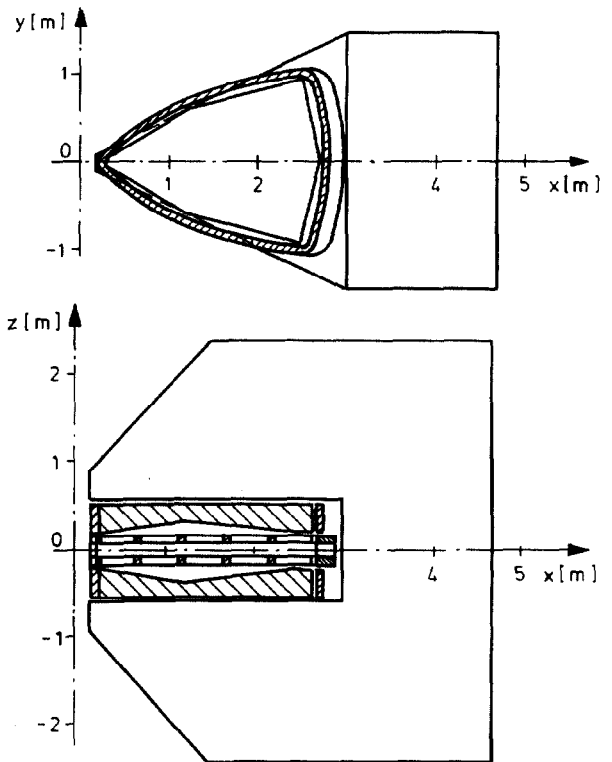


Fig. 2 Cross sections through a magnet.

## 2. The Superconducting Sector Magnets

Each of the 4 sector magnets (Fig. 2) consists of two superconducting main coils (4 tn), two superconducting layers of trim coils (2 tn), a warm iron yoke (300 tn) and two cold iron poles (10 tn). The shape of the main coils, the pole pieces and the yoke were optimized to achieve minimum deviations from a constant radial dependence of the average field  $B(r)$  in the range  $0.40 < r < 2.40$  m. Fig. 3 shows  $B(r)$  for maximum current (curve a) and half maximum current (curve b) in the main coils, both without trim coils. At the injection and extraction radius  $r_1 = .40$  m and  $r_2 = 2.40$  m additional field contributions are needed. A comparison between curve a) and b) shows the different influence of the magnetisation of the iron, which also has to be corrected.

Both these corrections and in addition the relativistic field increase are achieved by means of two superconducting trim coil layers, each consisting of 12 single coils as shown in Fig. 4. A fit program, which uses the computer code GFUN3D<sup>2</sup> for field calculations, gives the currents in the main coils and the trim coils. Fig. 5 shows two calculated field shapes. The deviations from the isochronous fields are less than  $\Delta B < 5 \cdot 10^{-3}$  T.

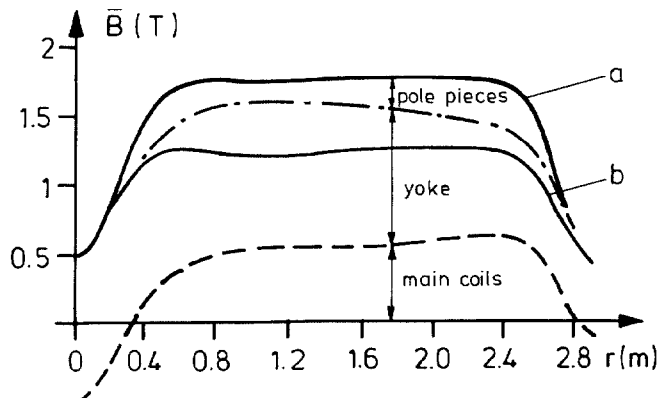


Fig. 3 Average field  $\bar{B}(r)$  for maximum (a) and half maximum (b) current in the main coils, both without trim coils. Contributions of the yoke, pole pieces and main coils are also shown.

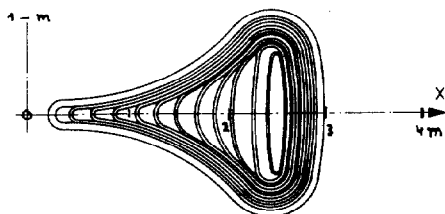


Fig. 4 Trim coil configuration

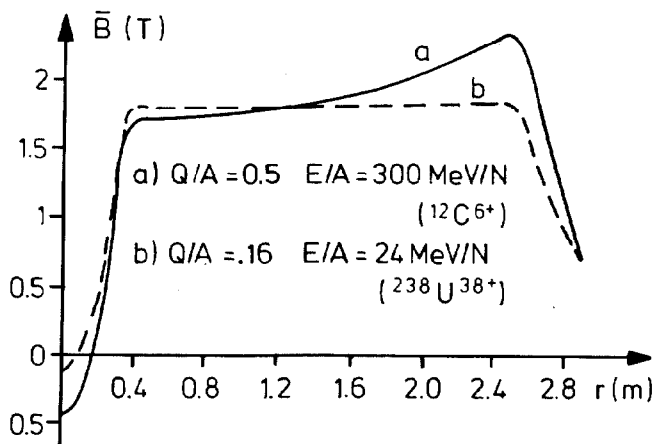


Fig. 5 Average field produced by the magnets including the trim coils for two different ions.

Each of the main coils consists of 23 double pancakes. Each d.panc. is build up of 26 windings of a rectangular hollow composite cable as shown in Fig. 6. The coil formers and reinforcements are made of strong aluminum alloy. The insulation of the potted coils is matched so that the coil former prestresses the coil when cooled down. The coil former is cooled by means of pipes with forced flow two phase helium at 4.5 K, 1.2 bar. Thus all heat from outside is screened. The helium inside the conductor (4.5 K, 1.4 bar) serves as a heat sink in case of a sudden heat input inside the coils.

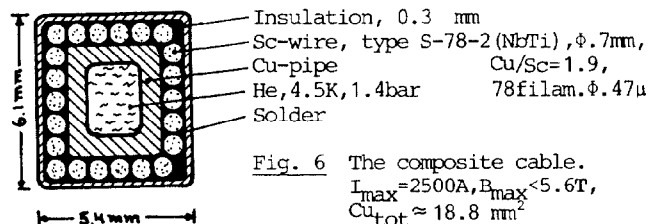


Fig. 6 The composite cable.  
 $I_{\max}=2500A, B_{\max}<5.6T,$   
 $Cu_{\text{tot}} \approx 18.8 \text{ mm}^2$

The stresses in the coil former and reinforcements are calculated in detail by the finite element method. They are below the elastic limit. The radial, outward directed forces acting on the main coils as a whole ( $\approx 3 \cdot 10^6$  N) are taken up by rods from the warm yoke. The vertical forces acting between the upper and lower coil packages are balanced by cold blocks inside the injection and outside the extraction radius. The vertical and radial forces on the cold poles are less than the forces on the coils.

In case of a quench of one magnet all others have to be deenergized too. If the stored energy per magnet of  $\approx 25$  MJ is distributed throughout the whole volume of the main coils (conductor only), the maximum temperature is less than 110 K. In order to insure uniform heating the total coils have to become normal conducting already at the early beginning of the quench. This is achieved by the following automatic protection system. The main coils of each magnet are divided into two equal parts L with a high mutual inductance M. The two coil parts L are connected to dump resistances  $R_1$  and  $R_2$  with  $R_1 \ll R_2$  (see Fig. 7). When disconnecting the power supply the currents  $I_1$  and  $I_2$  in the two circuits change from  $I_1 = I_2$  to the ratio:  $I_1/I_2 = R_2/R_1$  with a very short time constant

$$\tau = [1 - (\frac{M}{L})^2] \cdot \frac{L}{R_1 + R_2} \approx 0.01 \text{ sec}$$

The sudden change of the currents induces eddy currents in the copper parts of the conductor increasing the temperature above 10 K.

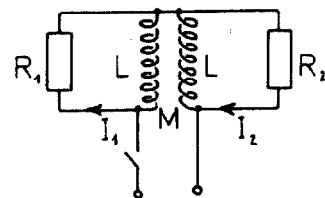


Fig. 7 Circuit for automatic quench protection

In August 80 one main coil (scale 1:1) has been ordered<sup>\*)</sup>. It will be delivered in November 1981 and then tested in our laboratory.

### 3. The RF-System

The RF-system consists of two cavities positioned in opposite valleys between the magnets. The cross section of one cavity is shown in Fig. 8. It is excited in the TE 101 mode with the maximum accelerating voltage  $U(r_2) = 1$  MV at extraction. This condition determines the length of the cavity ( $a = 3.55$  m). Because of the reduction of the cross section at small radii the accelerating voltage decreases faster than sinusoidally toward the center. In order to get  $U(r_4) > .25$  MV at injection the cavity is extended into the neighbouring valleys.

<sup>\*)</sup> Brown + Boveri (Mannheim, FRG)

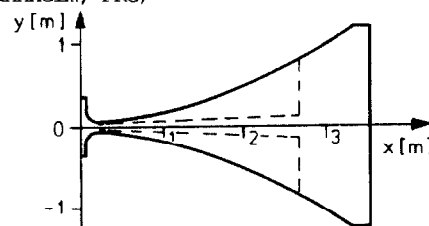


Fig. 8 Cross section of one cavity.

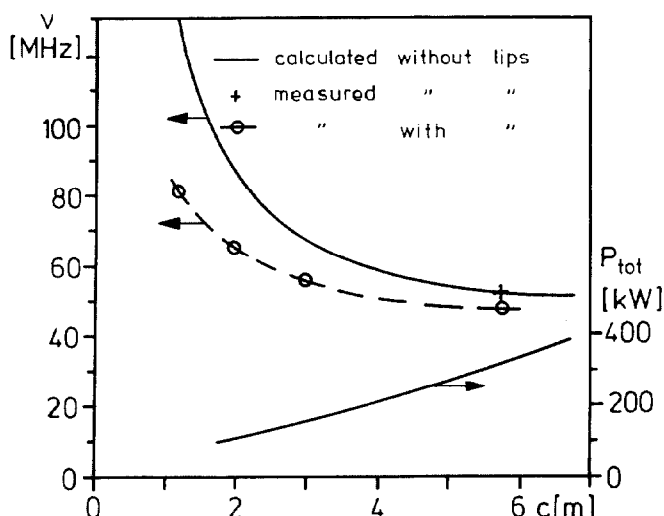


Fig. 9 The frequency of one cavity and the total power consumption in dependence of the cavity height  $c$ .

Fig. 9 shows the frequency and the power consumption of both cavities in dependence of its height  $c$  as calculated by a computer program for a cavity without inserted lips limiting the angle of the accelerating gap  $2\Delta\varphi$ . The power consumption curve favours the use of high harmonics of acceleration. Ions with the highest revolution frequency  $\nu_p = 13.1$  MHz could be accelerated on the 6. harmonic leading to 78.6 MHz ( $\approx c = 2.35$  m) as highest RF-frequency. The lowest RF-frequency is needed for the slowest ions with  $\nu_p = 3.1$  MHz. It is determined by the highest tolerable harmonic number. This number should not exceed 16 due to the increasing requests on magnet tolerances. Thus we need a RF-frequency range of 78.6 MHz  $< \nu_{RF} < 49.6$  MHz.

In the case of the higher harmonic numbers  $h$ , lips for limitation of the transition time have to be inserted. With lips as indicated by the broken lines in Fig. 8 we have measured on a model (scale 1:8) reduced frequencies and a more flat dependence of the height  $c$  (circles in Fig. 9), which can be explained by the capacitive load. In addition the capacitive load reduces the shunt impedance  $R$ , especially at high frequencies (low height  $c$ ).

The cavity has to be optimised for minimum power consumption, which is given by

$$P = \frac{U_{acc}^2}{2R(\Delta\varphi, c)} \cdot \left( \frac{h \Delta\varphi}{\sin(h\Delta\varphi)} \right)^2$$

The maximum accelerating voltage  $U_{acc} = 1$  MV per cavity is needed for the fastest ions ( $h=6$ ,  $\nu_{RF} = 78.6$  MHz). For this case  $P$  has to be minimized by an appropriate choice of  $\Delta\varphi$  and  $c$ . From preliminary measurements on the model it follows, that this minimum is obtained with small lips or no lips at all. It is expected to be less than 100 kW per cavity. In the case of higher harmonics  $\Delta\varphi$  has to be reduced resulting in additional losses. However simultaneously the accelerating voltage  $U_{acc}$  needed for constant turn separation can be reduced as  $1/\nu_p$ . Therefore adjustable lips are favorable.

Thus there are several possibilities to cover the required frequency range: changing the height  $c$  or the capacitive load or both methods combined. If the central wall between both cavities is removed, which can be done when using even harmonics only, they can be driven by one single amplifier, and the power consumption is reduced by  $\approx 20$  %.

#### 4. Beam matching and injection

The beam transfer line between the tandem Van-de-Graff and the cyclotron has been designed to achieve optimal beam properties. The layout is shown in Fig. 1.

The time structure of the beam is preformed by a low energy buncher, positioned in front of the tandem accelerator. This buncher, operating on a subharmonic of the cyclotron frequency, produces pulses at the terminal-stripper (TS) with a time width of about 300 ps for  $^{12}\text{C}$  and 1500 ps for  $^{238}\text{U}$ . The high energy buncher (B) after the tandem provides an image of this time focus at the post-stripper (PS). Due to the different effective lengths for light and heavy ions between the terminal stripper and the high energy buncher the time width at the post-stripper reduces to 80 and 200 ps for light and heavy ions, respectively. The magnetic beam line system between the buncher and the post-stripper is to first order achromatic, leading to decoupled phase spaces and sharp focusses in all dimensions at the post-stripper. This ensures a minimum increase of the emittances due to angular and energy straggling in the stripper foil.

After the post-stripper the beam is transposed to point A in an S-shaped beam line formed by four  $90^\circ$ -bending magnets. This part of the beam line is again achromatic with a unit transformation matrix for the horizontal and vertical phase space. In the longitudinal direction it acts as a "negative drift length". Particles with higher than the central momentum travel a longer distance inside the dipole magnets and therefore arrive later at point A. The length of this negative drift can be adjusted such that it cancels the effective length of the remaining system from point A to the first isochronous orbit in the cyclotron. This gives a unit transformation for the longitudinal direction between the post-stripper and the cyclotron. With this system the time focus at the stripper is reproduced in the cyclotron without an additional buncher which otherwise would be needed for refocussing. During acceleration in the cyclotron the time width of 80 to 200 ps is again reduced by a factor of four due to an increasing energy gain per turn<sup>3</sup>.

In the last section between point A and the cyclotron the emittance and dispersion matching of the beam will take place. This part can be designed in detail when the injection inside the cyclotron is completed. It will look similar to the corresponding part of the beam line of the VICKSI - accelerator in Berlin<sup>4</sup>.

The design of the injection system inside the cyclotron is in progress. It consists of one electrostatic septum and four superconducting coils, positioned in the tip of each magnet between the trim coil layers. Two coils in neighbouring sectors are used for deflection of the incoming beam. The other two serve as compensation for the first harmonic field distortion. The central region of the cyclotron is kept free for the RF-cavities. The beam is injected radially through the valley between two sector magnets. As the field in that region does not scale with the average field level, the incoming beam has to be shielded to achieve a constant trajectory. There are several concepts in discussion for this purpose.

#### References:

- 1) SuSe-Group, IEEE Trans.Nucl.Sci. NS-26, No 3 (1979) 3721
- 2) A.G.A.M. Armstrong et al., Report RL-76-029/A(1976)
- 3) W. Joho, Part. Accel., 6 (1974) 41
- 4) G. Hinderer and K. H. Maier, IEEE Trans. Nucl. Sci. NS-22, No 3 (1975) 1722.